REPORT DOCUMENTATION PAGE

AFRL-SR-BL-TR-00-

38

05*40*

1. REPORT DATE *(DD-MM-YYYY)*	2. REPORT TYPE	3. DATES COVERED *(From - To)*
8/15/00	Final	April 97 – March 98

4. TITLE AND SUBTITLE	5a. CONTRACT NUMBER
Quasi-optical Pulse Formation using Triangular Arrays of Josephson Junctions	
	5b. GRANT NUMBER F49620-97-1-0269
	5c. PROGRAM ELEMENT NUMBER

6. AUTHOR(S)	5d. PROJECT NUMBER
Orlando, Terry P.	
	5e. TASK NUMBER
	5f. WORK UNIT NUMBER

7. PERFORMING ORGANIZATION NAME(S) AND ADDRESS(ES)	8. PERFORMING ORGANIZATION REPORT NUMBER
Massachusetts Institute of Technology **77 Massachusetts Avenue** **Cambridge, MA 02134-4307**	

9. SPONSORING / MONITORING AGENCY NAME(S) AND ADDRESS(ES)	10. SPONSOR/MONITOR'S ACRONYM(S)
Dr. Harold Weinstock **AFOSR/NE** **110 Duncan Avenue, Suite B115** **Bolling AFB, D.C. 20332-0001**	
	11. SPONSOR/MONITOR'S REPORT NUMBER(S)

12. DISTRIBUTION / AVAILABILITY STATEMENT

Approved for public release; distribution unlimited

13. SUPPLEMENTARY NOTES

20001023 057

14. ABSTRACT

A Josephson oscillator array was investigated through both DC and AC experiments. The simulations and analysis of Yukon and Lin suggested that arrays with three junctions per cell might have unique advantages as high frequency oscillators. These triangular arrays operate with a bias flux of half a flux quantum and power is coupled from the horizontal junctions. This configuration allows one to couple from a whole series of junctions that oscillate in-phase. The power was successfully measured from the horizontal junctions by two different methods. In collaboration with Dr. Cawthorne and Professor Lobb at University of Maryland, an on-chip detector junction was used and Shapiro steps were measured. Also, in collaboration with Dr. Caputo and Professor Ustinov at KFA in Juelich, Germany, a finline antenna was placed across the horizontal row of junctions and coupled power off-chip, to a room temperature receiver. Both experiments demonstrated a proof-of-concept, and future work should include improved matching to measure the maximum available power.

15. SUBJECT TERMS

Superconducting Electronics

16. SECURITY CLASSIFICATION OF: U			17. LIMITATION OF ABSTRACT	18. NUMBER OF PAGES	19a. NAME OF RESPONSIBLE PERSON **Terry P. Orlando**
a. REPORT **U**	b. ABSTRACT **U**	c. THIS PAGE **U**	U	15	19b. TELEPHONE NUMBER *(include area code)* **617-253-5888**

DTIC QUALITY INSPECTED 4

Standard Form 298 (Rev. 8-98)
Prescribed by ANSI Std. Z39.18

Quasi-optical Pulse Formation Using Triangular Arrays of Josephson Junctions

F08671-97000989

1 April, 1997 — 31 March 1998: Final Report

Terry P. Orlando

Department of Electrical Engineering and Computer Science

Massachusetts Institute of Technology

77 Massachusett Ave., Bldg. 13-3006

Cambridge, MA 02139-4307

phone: 617-253-5888

fax: 617-258-6640

email: orlando@mit.edu

August 17, 2000

2. Goals

The goals and objectives of this work were:

1. Fabricate and measure triangular arrays of superconducting Josephson junctions which are connected in a phase-locked manner, both within a circuit and quasi-optically.

2. Test the idea proposed by Yukon and Lin to produce guided pulses of microwave radiation from quasi-optically connected arrays of superconducting Josephson junctions.

This work was to be done over a three year period; but it was only funded for one year. Nevertheless, we were able to make significant progress on these goals.

3. Executive Summary

1. We have measured the DC characteristics of discrete single-row and single-cell triangular Josephson junctions. These samples were designed by us and fabricated by Hypres, Inc. in niobium trilayer technology. We observed two resonant steps in the current-voltage characteristics that have been predicted by Yukon and Lin and Barahona *et al.* These steps correspond to the LC-resonances where L is either the self-inductance of the cell or the inductance of the horizontal Josephson junction and C is the capacitance of the junctions.

2. Ac power at 75 GHz were measured in the Ustinov's laboratory in Germany. The radiation was coupled out of the array by fin-line antennas and was detectable at the predicted frequency, although the power itself was low due to impedance mismatch. Furthermore, the power was maximized when a half a flux quantum was in each cell of the array.

3. The above DC and AC measurement confirm the predictions of Yukon and Lin about the basic operation of triangular arrays of Josephson junctions.

4. Publications

"Experiments with Triangular Arrays of Josephson Junctions," P. Caputo, A.E. Duwel, T.P. Orlando, A.V. Ustinov, N.C.H. Lin, and S.P. Yukon, Proceedings of the ISEC, Berlin, Volume 3, page 180, 1997.

"Harmonic Resonances in Nonlinear Josephson Junction Circuits: Experimental and Analytical Studies," by A. E. Duwel, Ph.D. Thesis, Massachusetts Institute of Technology, June 1999.
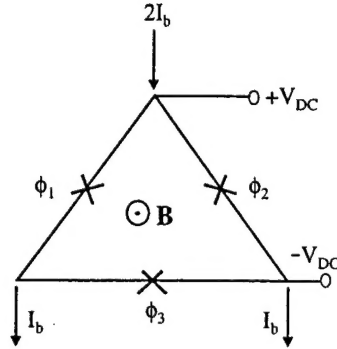
Figure 5-5: A single triangle cell.

5.2 Triangular Arrays

5.2.1 DC Measurements

Triangular arrays have been proposed as a possible alternative for obtaining useful AC power from Josephson networks A single triangular cell is shown in Fig. 5-5. DC current is applied to the vertical junctions, and the average DC voltage V_{DC} is measured across the vertical junctions. A row of triangular cells is shown in Fig. 5-6.

According to the analysis of Yukon and Lin, strong L_sC and L_JC resonances can occur in systems with three junctions per cell. The L_sC resonance is similar to that associated with the Eck step in parallel arrays. There is no counterpart of the L_JC resonance in parallel arrays, since it is related to the presence of the new third junction, which receives no DC bias [1] These resonances correspond to large-amplitude AC oscillations of the junction voltages. The phase differences between the oscillating junctions are determined by the magnetic field, just as for the case of parallel (2 junction/ cell) arrays. At $f = 1/2$, adjacent vertical junctions oscillate

---

[1] We call the junctions in triangular arrays which receive no DC bias "horizontal" and the junctions which receive a DC bias "vertical", since, in this thesis, the DC bias is usually drawn in the vertical direction on the page.
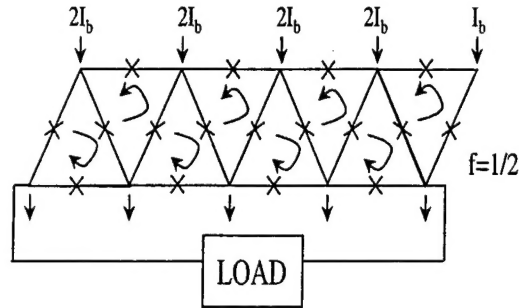
3

Figure 5-6: Triangular cell row, with load connected across horizontal junctions. Bias resistors are used to inject the current. The directions of the circulating currents at $f = 1/2$ are shown.

exactly out-of-phase. However, it is the relative phases of the horizontal junctions which are of interest in this system. Yukon and Lin used numerical simulations to show that at $f = 1/2$, the horizontal junctions along the same line oscillated exactly in-phase. This in-phase oscillation is stabilized and tuned by the DC bias on the vertical junctions. For example, in Fig. 5-6, all of the horizontal junctions along the bottom of the row oscillate in-phase. Therefore, the authors suggested connecting a load across the *horizontal* junctions, as shown in the figure. For N_h horizontal junctions, this supplies N_h times the voltage of a single junction to the load. If the load is either matched to or voltage-biased by the array, the delivered power will be multiplied by N_h. Since the voltage-bias regime corresponds to the case where the source impedance (the array) is much less than the load impedance, this is where typical systems (50 Ω loads) might operate.

The DC IV curves of a single cell and an 8-cell array (unloaded) are shown in Fig. 5-7. For both the single cell and the array, the parameters are $\beta_c = 230$ and $\Lambda_J^2 = 2.4$. The lower voltage step is associated with an $L_J C$ resonance, while the upper step is associated with an $L_s C$ resonance The currents are normalized to
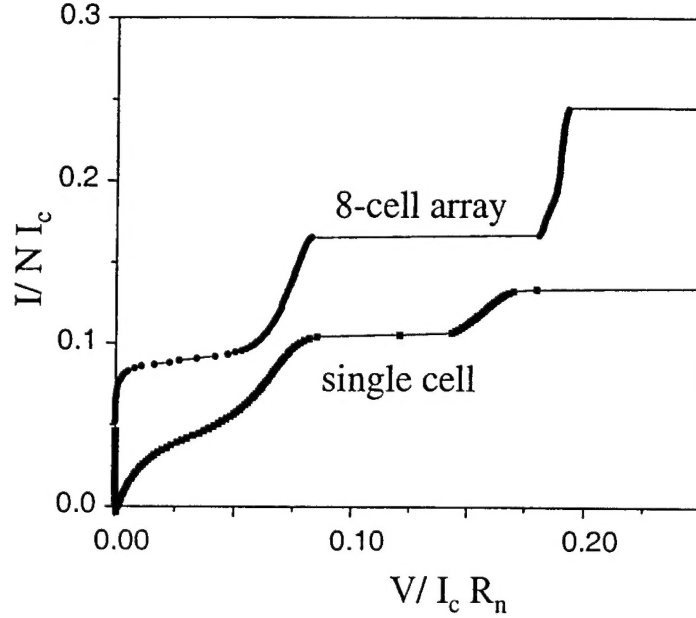
Figure 5-7: Current-Voltage characteristics of a single triangular cell and of an 8-cell array. The parameters are $\beta_c = 230$ and $\Lambda_J^2 = 2.4$, and $f = 0.5$.

the number of vertical junctions so that the systems can be compared. The observed steps are characteristics of single cells, and their position does not change significantly with the number of array cells. Measurements of two different cell sizes, however, show that the upper step voltage depends strongly on the cell geometry, while the lower step is only slightly affected. The steps appear only in the presence of a magnetic field, when the average applied flux per cell is approximately one-half. They are stable for a range on $f = 0.3 - 0.7$. Figure 5-8 shows the range of stability and the step voltage variation, by plotting the step voltage together with the array critical current versus frustration. Both are periodic in field. As usual, the critical current is largest at $f = 0$, while the steps maximize at $f = 0.5$. These steps also appear in measurements of high critical current density junctions, where $\beta_c \approx 10 - 20$. At low temperatures the high current density samples have Λ_J^2 values well below 1. We found that the upper step, corresponding to the $L_s C$ resonance, is only stable when the temperature is raised such that $\Lambda_J^2 > 0.3$ (approximately).
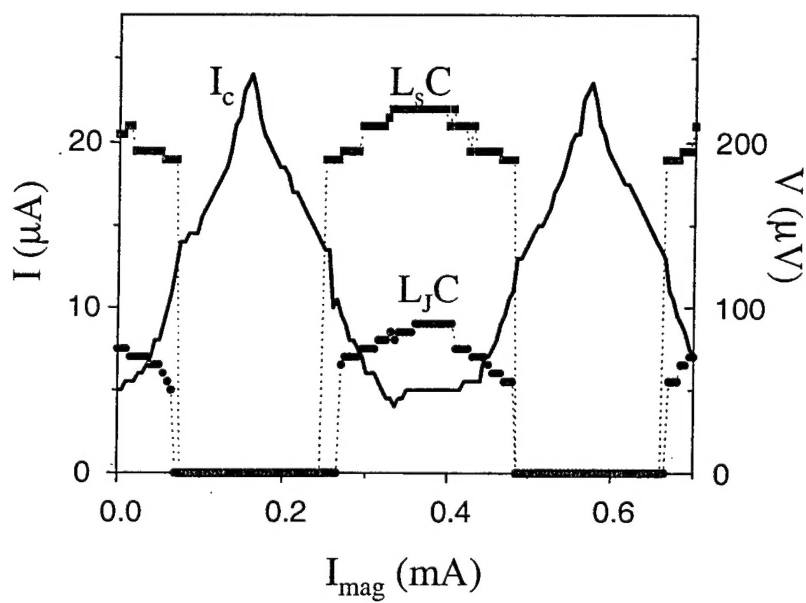
Figure 5-8: Step voltage versus field is compared to the critical current versus field for the 8-cell triangular array.
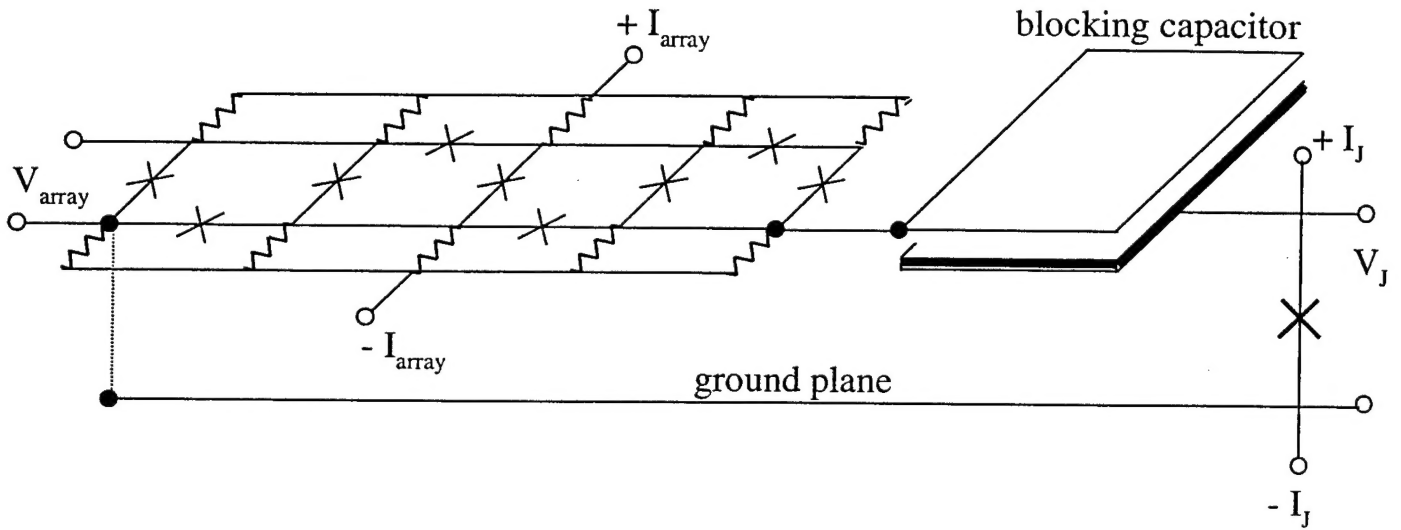
Figure 5-9: Triangular array coupled to a detector junction.

5.2.2   AC Measurements: on-chip and off-chip

DC measurements have confirmed the presence of an L_sC resonance in the triangular cell arrays. The AC power from horizontal junctions has been successfully tested two different ways. Both detection methods involved collaborations with other groups.

The AC output of a Josephson array can be detected on-chip by using another Josephson junction. If AC power at a single frequency is coupled into a single over-damped junction, then Shapiro steps   will appear in the detector junction IV characteristic. The voltage position of the step is related to the AC bias frequency by the Josephson relation. Likewise, the AC bias frequency is determined by the DC bias of the Josephson junction array source. The height of the step is related to the power of the radiation. By simulating a single Josephson junction and the coupling circuit to an ideal AC source (which in this case represents the triangular row), the power coupled out from the array can be estimated. This scheme was first successfully used on Josephson networks by Benz   and was later improved by Cawthorne [66].

Our preliminary measurements of the AC power from a triangular row use the

7

exact coupling circuit and detector junction designed by Professor Lobb and Fred Cawthorne at the University of Maryland, Department of Physics. Their original system was also fabricated by HYPRES, and their results on 2D square arrays are published in reference . A schematic of the triangular array coupled to a detecting junction is shown in Fig. 5-9. The arrays measured have 20 cells, or 10 horizontal junctions. The blocking capacitor has dimensions $376 \times 181\ \mu m^2$ and has a capacitance of approximately $C_B = 14$ pF. A ground plane is placed under the array to decrease the self inductance of the loops and to provide a low-inductance connection from the array to the detector. The ground plane is narrowed to a strip under the blocking capacitor, as suggested by Cawthorne $et\ al.$ in [66], leading to a parasitic capacitance from the blocking capacitor to ground of only $C_G = 0.5$ pF. Both the detector junction and the array junctions are $3 \times 3\ \mu m^2$ and are shunted with approximately $R_{sh} = 1.1\ \Omega$. For $j_c = 1300\ A/cm^2$, this gives an overdamped system with $\beta_c = 0.15$. We estimate the loop inductance as roughly $L_s \approx \mu_o\sqrt{A}/3.7$, where A is the loop area and the factor of 3.7 is due to the ground plane . With the loop area $A = 18 \times 18\ \mu m^2$, $L_s \approx 6.2$ pH. Thus, $\Lambda_J^2 = 0.45$. Due to the presence of a ground plane, magnetic field must be applied to the array using a control wire. The wire is not included in the schematic of Fig. 5-9, but is placed along the line of the top row of horizontal junctions and is superconducting.

Using measurements of the array critical current versus field, as in Fig. 5-8, we determine that the value of $I_{ctrl} = 0.92$ mA in the control wire produces $f = 1/2$ in the array. Since these arrays are overdamped, the L_sC and L_JC resonant steps are not very pronounced and cannot be used to determine f. When the array is biased at a nonzero voltage and $f = 1/2$, the theory and simulations of [49, 50] indicate that the horizontal junctions should oscillate in-phase and couple power to the detector. This is confirmed by the observation of Shapiro steps in the detector junction. Figure 5-10 shows the detector junction IV curves for both $I_{array} = 0$ and $I_{array} = 6.6$ mA. When $I_{array} = 0$ mA, no Shapiro steps appear. Other structure is visible in the IV curve, resulting from the dynamics of the single junction with the load that it sees. In the IV curve on the right, a clear step appears at $V_J = 0.41$ mA. The dotted
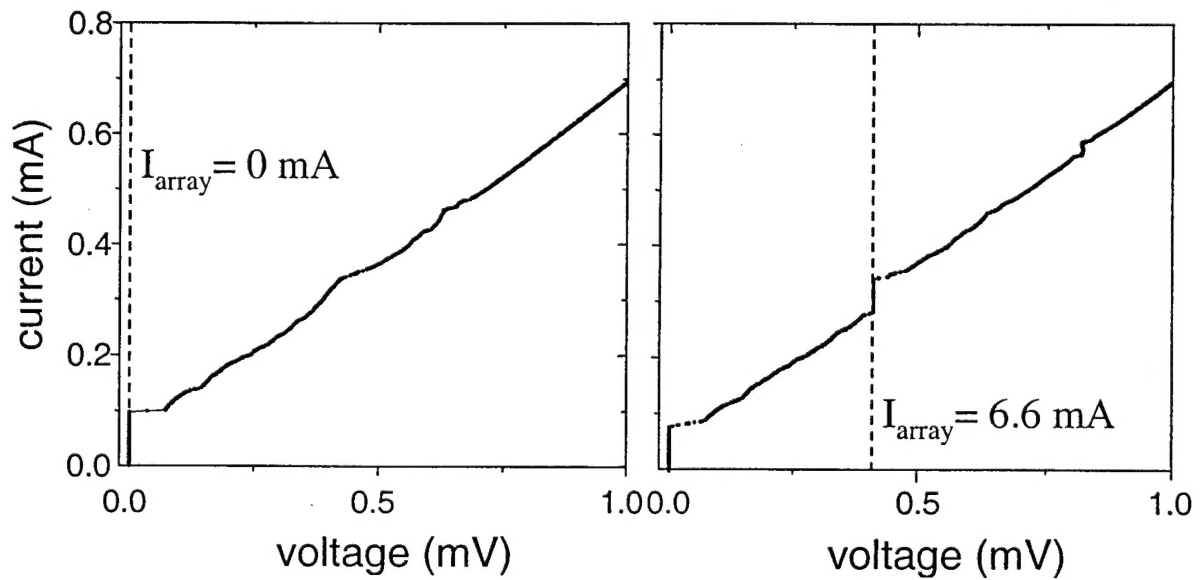
Figure 5-10: IV curves of the detector junction when the triangular array is biased at $I_{array} = 0$ mA, in the left IV, and $I_{array} = 6.6$ mA, on the right. The dotted line shows the measured array voltage, which also matches the voltage of the primary Shapiro step. For $I_{array} = 6.6$ mA, the primary Shapiro step occurs at $V_J = 0.41$ mV, and a second step is visible at $V_J = 0.82$ mV.

line shows the measured voltage across the triangular array when it it biased with $I_{\text{array}} = 6.6$ mA. The fixed array voltage exactly matches the voltage of the Shapiro step. A second Shapiro step is also visible at $V_J = 0.82$ mA. When the array voltage is moved (by changing I_{array}), the Shapiro step in the detector junction also changes.

Figure 5-11 shows an IV of the triangular array at $f = 0$. (Due to the large damping, there is no visible change in the array IV as f is increased, and the step associated with the L_sC resonance in underdamped arrays is not visible). The region within the dotted lines indicates the range of array bias values which produce a measurable Shapiro step in the detector junction. The voltage range corresponds to a bandwidth of $24 - 227$ GHz. This wide range implies that the array produces AC power even when not biased at a particular resonance voltage. However, the height of the Shapiro step varies within the bandwidth of Fig. 5-11, and the power which can be coupled from the array is not uniform within that bandwidth. To estimate the power which is coupled from the horizontal junctions of the array, numerical simulations of the detector junction should be matched to the IV curves of Fig. 5-10. On the other hand, direct measurements of the power can be obtained using off-chip detectors.

Off-chip detection is usually more desirable, since then linewidth measurements are also possible. We collaborated with Dr. Pasquilina Caputo and Professor A. Ustinov [2] at the Institute for Thin Film and Ion Technology at KFA in Juelich, Germany to assist with designs for off-chip detection. The laboratory at KFA was equipped with a cryogenic probe with rectangular waveguides for the frequency range of $80-120$ GHz. The room temperature receiver is operated as a radiometer with a fixed detector bandwidth. The power from the triangular row is coupled into the rectangular waveguide via a finline antenna. The exponentially tapered finline antenna transforms a stripline impedance into a rectangular waveguide [80]. A schematic of the design is shown in Fig. 5-12. In the figure, $M0 - M3$ are superconductor layers of the HYPRES process. In order to obtain a good impedance match, the stripline impedance Z_s at the input of the antenna was calculated in the limit when the stripline width w is

---

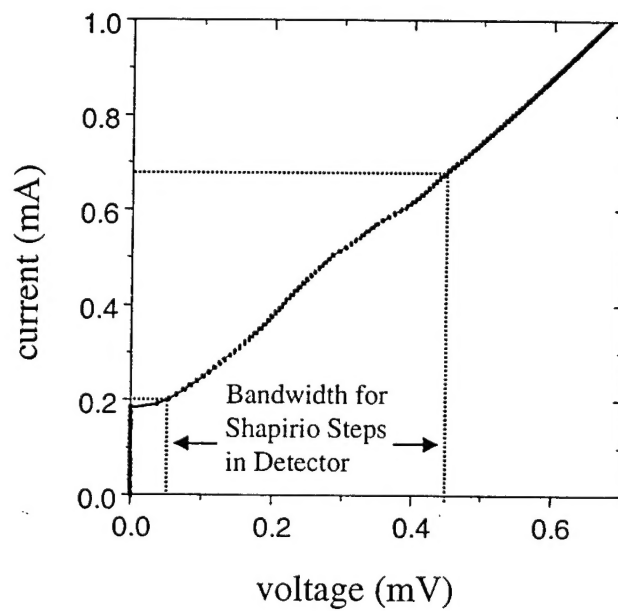[2]Present address: University of Erlangen, Germany.

Figure 5-11: IV curve of the triangular array, when the detector junction is left unbiased. The region within the dotted lines indicates the range of bias for which Shapiro steps can be measured in the detector junction. The range of voltages is $0.05 - 0.47$ mV, corresponding to a bandwidth of $24 - 227$ GHz.

larger than the dielectric height h ($w/h > 2$)

$$Z_s = \frac{377}{\sqrt{\epsilon_r}} \left(\frac{w}{h} + 0.883 + \frac{\epsilon_r + 1}{\pi \epsilon_r} \left[\ln \left(\frac{w}{2h} + 0.94 \right) + 1.451 \right] + 0.165 \frac{\epsilon_r - 1}{\epsilon_r^2} \right)^{-1}$$

where $\epsilon_r = 3.5$ is the dielectric constant for SiO_2 and $h = 0.65\,\mu m$ with HYPRES. In this calculation, the stripline is treated as a normal conductor. The width of the stripline was then chosen to match the impedance looking into the triangular row. A 12-cell row was used, coupling 6 horizontal junctions across the antenna electrodes. The impedance of the array was calculated by replacing the junctions with parallel R_nC circuits. Much better models for the junction impedance are now available [51]. However, this effort at impedance matching sufficed for our preliminary experiment. The high current density junctions ($j_c = 1000\,A/cm^2$) with areas of $3 \times 3\,\mu m^2$ have an impedance of approximately $4\,\Omega$ at 100 GHz. In this model, then, the array impedance is $24\,\Omega$ at the expected operating frequency. Therefore a stripline width of $w = 5\,\mu m^2$ was chosen for the start of the finline antenna.

Figure 5-13 shows the measurements by Dr. P. Caputo at KFA of the power versus the triangular array bias at $f = 1/2$. Radiation is detected at 75 GHz when the array is biased on the L_sC resonance step. The detector bandwidth is 0.9 GHz, but is wider than the peak in Fig. 5-13. The radiation is a maximum at $f = 1/2$ and decays to zero at $f = 0, \pm 1$. This shows that, as predicted by Yukon and Lin the applied field can change the relative phases of the horizontal junctions. The detected power is a maximum when the horizontal junctions are oscillating in-phase at $f = 1/2$. The maximum power from the array is estimated to be 90 pW, after taking into account losses (≈ 13 dB) in the finline antenna and waveguide coupling.
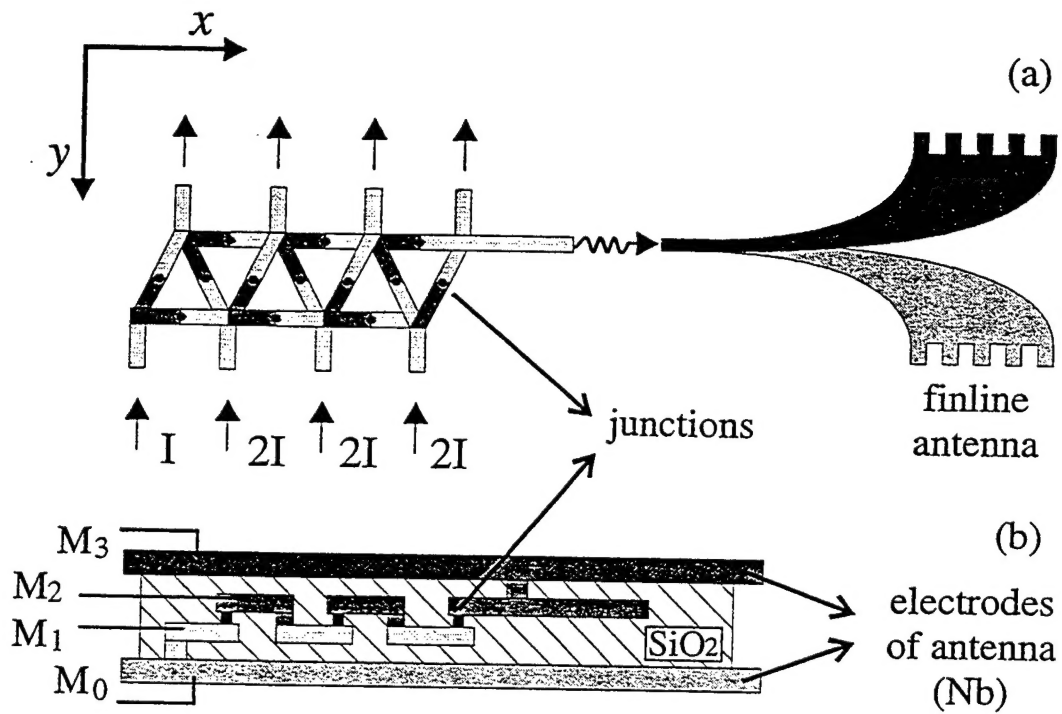
Figure 5-12: (a) Schematic top view of a 6 cell triangular array with the finline antenna which couples the array signal to the $80 - 120$ GHz rectangular waveguide, and (b) cross-sectional view of the horizontal junctions of the array inserted in the microstripline and ending in the antenna.
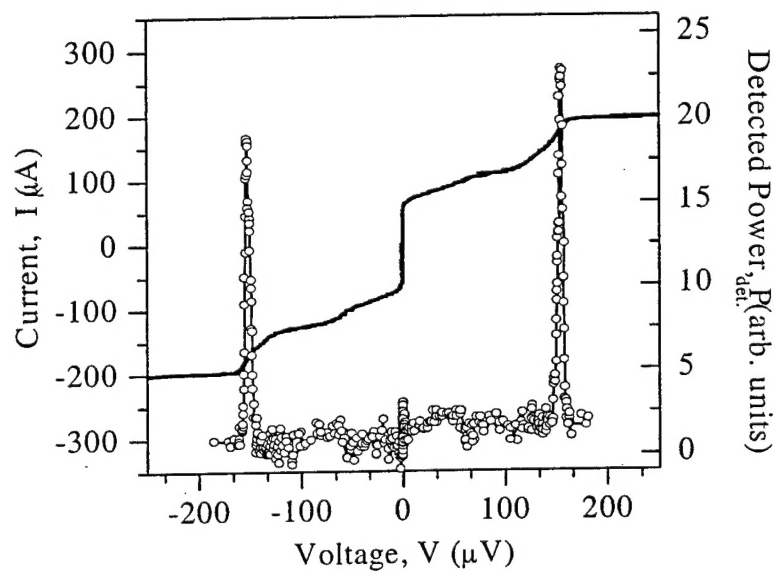
Figure 5-13: Measurement by Dr. P. Caputo of radiation emission from a 12 cell array. The IV curve is shown together with the detected radiation power at frequency 75 GHz. The detector bandwidth is 0.9 GHz.